DFG-SPP-1207 „Strömungsbeeinflussung in Natur und Technik“.
DFG SI 1542/1 “Analysis of the relation between skin morphology and local flow conditions for a fast-swimming dolphin“.

Vadim Pavlov[1], Donald Riedeberger[2], Ulrich Rist[2], Ursula Siebert[1].

1. Institute of Terrestrial and Aquatic Wildlife Research, University of Veterinary Medicine Hannover, Foundation, Werftstr. 6, 25761 Büsum
2. Institute of Aerodynamics and Gas Dynamics, University of Stuttgart, Pfaffenwaldring 21, 70550 Stuttgart

E-mail: pavlov.v.v@gmail.com

Summary

The dolphin skin close to the anisotropic compliant wall design could potentially reduce the friction drag. The goal of this work was to study the relation between local flow conditions around dolphin model and parameters of skin morphology relevant in flow/skin interface. Three-dimensional CAD models presenting authentic geometry of fast-swimming common dolphin *Delphinus delphis* and low-swimming harbor porpoise *Phocaena phocaena* were constructed. CFD study of the flow parameters were carried out for the natural range of dolphin swimming velocities. The results of this study allow to conclude that the streamwise variability of the dolphin skin structure appears to be associated with the streamlined body geometry and corresponding gradients of the velocity and pressure rather than with specific local Re numbers. The hypotheses on different optimal conditions for potential drag-reducing properties of dolphin skin are proposed.

Introduction

The basic idea of biomimetics or bionics is to develop new technologies based on highly effective and specialized solutions found in nature. Fast moving animals are usually optimized for efficiency by evolution. Since marine top predators move within a high density and therefore high drag and high buoyancy medium, their need for efficient drag reduction mechanisms appears quite evident. Modern engineering designs of marine and air transport vehicles make use of streamlined shapes to reduce the form or pressure drag while several solutions aimed at reducing friction drag came from the study of sea animals.

Dolphins are one of the most famous examples of extreme adaptations to drag reduction. Interest in the understanding of a dolphin's hydrodynamics was initiated by Sir J Gray who published his analysis of a dolphin's energetics with unexpected outcome, later called Gray's paradox [1]. Assuming a fully turbulent flow Gray came to the conclusion that a dolphin should possess either enormously powerful muscles (seven times more power per unit mass than any other mammalian) or must be capable of maintaining laminar flow by some extraordinary means. In the late 1950s the aerodynamicist Max Kramer claimed that a dolphin ensured a low level of friction drag by maintaining laminar flow over most parts of its body. The dolphin's skin having an unusually ordered inner structure was considered to be a natural compliant wall effectively suppressing the growth of Tollmien-Schlichting waves in the transition region of the flow, Kramer [2], [3]. This suppression delays the transition from laminar to turbulent flow in the boundary layer thus decreasing the friction drag. Kramer proposed the drag-reducing properties of a dolphin's skin as a solution of Gray's paradox and initiated numer-

ous investigations of the structure and function both of dolphin skins and compliant walls.

The structure of the dolphin skin presents morphological adaptations which appeared as a result of 50 millions year of evolution of cetaceans. A thick layer of skin covers the body of dolphins and streamlines his skeleton and muscles. The skin surface is smooth, hairless and elastic. Skin glands are absent with little exceptions only and the number of layers of the epidermis is reduced compared to other mammals, Sokolov [4].

The structure of the dolphin skin and the blubber layer is highly organized and complex (Parry [6], Sokolov [5], Aleyev [7], Haun et al. [8], Pershin [9], Toedt et al. [10], Hamilton et al. [11]). Unlike the chaotic arrangement for terrestrial mammals, the dermal ridges in cetaceans' skins are arranged in a highly ordered manner. This feature of dolphins' skin inspired suggestions of its possible relation with the flow direction (Sokolov [4], Palmer & Weddell [12], Purves [13], Surkina [14]). In addition, variable blood pressure in capillary vessels in the papillary and sub-papillary layers can modify the range of mechanical properties of the dolphin skin, Pershin [9].

The mechanical properties of dolphin skins related to species, position on the body, degree of training, and physical condition was investigated by Babenko et al. [15] or Toedt et al. [10], for instance. They found that the modulus of elasticity E was lower in the middle of the common dolphin compared to more anterior and posterior sections of the body [16]. For a freshly captured bottle-nosed dolphin, E was higher than for the same animal after training, when the dolphin was calm. The higher value of the modulus of elasticity was interpreted to better correspond to the condition of high-speed swimming [15]. The elastic properties of the integument are particularly dependent on the deeper layer of thick blubber. The blubber layer is highly resilient, with E-modulus similar to biological rubbers (e.g. Pabst et al. [17]).

Experimental studies of living dolphins did, however, not confirm Gray's supposition about fully laminar flow of swimming dolphin. Direct measurements of turbulence by means of transducers attached to the dolphin's body as well as visualization studies of the flow of swimming dolphins indicated turbulent boundary layers over the most part of the body (Romanenko [18], Rohr et al. [19]). Nevertheless, the level of turbulence measured in the boundary layer of swimming dolphins was significantly lower compared with the flow over a rigid or solid model of the dolphin (Romanenko [18]).

The state-of-the-art view of dolphin hydrodynamics assumes a number of simultaneous adaptations, e.g. to unsteady velocity and pressure gradients from accelerating water over the body, skin tension and micro vibrations, shedding of the

superficial layer of epidermis as well as skin damping, which provides additional boundary layer stabilization for the swimming dolphin (Gray [1], Haider & Lindsley [20], Ridgway & Carder [21], Babenko & Carpenter [22], Romanenko [18], Nagamine et al. [23]).

Considerable progress has also been achieved in the theoretical modeling and understanding of compliant walls and the current level of knowledge assumes a substantial delay of laminar-turbulent transition as well as drag reduction in a turbulent boundary layer by appropriately designed compliant walls (Gad-el-Hak [24], Choi et al. [25], Carpenter et al. [26]). According to these a two-layer anisotropic compliant wall which comes close to the actual dolphin's skin structure possesses the best drag-reducing properties (Sokolov [26], [4], Palmer & Weddell [12], Grosskreutz [28], Stromberg [29], Carpenter & Morris [30], Yeo [31]).

At the same time, the mechanism of dolphin skin/flow interaction is still unclear. There are several objective reasons: First, there is still a considerable lack of quantitative data of potentially drag-reducing features of dolphin skin morphologies. Second, these were rarely considered in connection to the local flow properties. The goal of this work is to study the relation between local flow conditions around dolphin model and parameters of skin morphology relevant in flow/skin interface.

Methods

Scheme of sampling.

The scheme of sampling was elaborated both for study of skin morphology and parameters of the flow simulated around the dolphin model. As the goal of the study was to compare the flow/skin interface in regions which are characterized by different Reynolds numbers, two parts of the body were selected for that purpose. The first is the dorsal fin that presents a typical wing-like shape and is built of symmetrical cross-sections. The second is limited by the tip of the melon on the head on one side and the position between dorsal fin and genital slit on the other side. Both regions present smooth streamlined bodies with similar geometry at different size. For the comparative purpose in both regions the sampling was done in 20 points located on equal intervals along a line on the body surface. The dimensionless scheme of sampling allowed comparison of the flow/skin interface for the different parts of the dolphin body.

Skin morphology and morphometry

The skin samples of 4x4x4 mm^3 in size were fixed in 10% formalin, dehydrated and embedded by the Technovit 7100 media. Both vertical cross-sections and sections parallel to the skin surface were made with the thickness of 7 mkm. Sections were dried and stained by hematoxylin-eosin for the general picture and aldehyde-fuchsin to reveal the elastic fibers in dermis layer of the skin.

All measurements of the skin features on the histological sections were done with a measurement system including an Olympus CK X41 microscope and morphometry software. The images of skin sections were captured by the video camera, calibrated, and saved in JPG file format. On the vertical cross sections of the skin the following parameters were measured:

1. Height of the epidermis (HEP), mm
2. Height of the dermal papillary layer (HDP), mm
3. Height of the subpapillary layer of dermis (HSL), mm
4. Thickness of the dermal ridges (TDR), mm
5. Thickness of the epidermal ridges (TER), mm

The angle between the dermal ridges direction and the long axis of the body was measured on sections parallel to the skin surface. The average values of all morphological parameters were calculated based on three repeated measurements.

CAD modeling

A full-scale, three-dimensional CAD model of a common dolphin *Delphinus Delphis* was constructed with SolidWorks software. For the common dolphin the measurements and photos of the body of a newly stranded animal were used. All measurements were taken according to the standard protocol of postmortem examination (Kuiken and Hartmann 1993). Laser scanning data of the rigid model of the same species held at the German Oceanographic Museum in Stralsund were used for correction of the dolphin's body geometry. The resulting model presents an authentic geometry of an adult female common dolphin of 1.94 m length.

Additionally, a three-dimensional geometry of a by-caught harbour porpoise was obtained by an Atos V7 optical scanning system by IGS Development GmbH. Scanned data were processed with the GOM software and exported in CAD format as a set of cross-sections. The resulting model built with the SolidWorks software presents an authentic geometry of a sub-adult male harbor porpoise of 1.1 m length.

For both species models of fins were constructed separately using photos of fin outlines as well as cross-sectional measurements of fins and joined to the models of the bodies. A straightened body position, which corresponds to the gliding phase of the dolphin's swimming cycle, was chosen for the CFD study.

CFD study

The flow around the dolphin and porpoise model was studied with the FloWorks software. The flow parameters along with both sampling lines on the common dolphin were measured for the range of natural swimming velocities.

The calculations were done under the following conditions: Static pressure 101325 Pa, temperature 20° C, turbulence intensity 0.1%, and turbulent length scale of 3.44E-04 m. The velocity in X direction (along long axis of the model) varied from 2 to 8 m/sec at fixed 0 m/sec for the velocity both in Y and Z direction. FloWorks uses the finite volume method to solve the Reynolds-averaged Navier–Stokes equations, implementing the k − ε turbulence model.

The numerical simulation of laminar-turbulent transition on the same model of common dolphin using the empirical γ-Re_θ transition model was carried out by Donald Riedeberger [32] at IAG, Stuttgart University. The finite-volume code STAR-CCM+ was used with a RANS formulation and SST-k-ω closure together with similar boundary conditions as prescribed before. Simulated swimming speed varied in the range from 0.25 to 5 m/sec, with the turbulent intensity ranging from 0.25% to 5%.

Model of the flow/skin interface

The simplified model of the flow/skin interface includes the angle ϕ formed by the velocity vector on the outer edge of the boundary layer and the plane of the dermal ridges. The angle α formed by the dermal ridges with the Y-axis was used for the calculation of a 2D vector of dermal ridges. Then a 3D vector ***a*** of the dermal ridges was obtained by the projection of the 2D vector on the surface of the 3D model (Pavlov 2003).

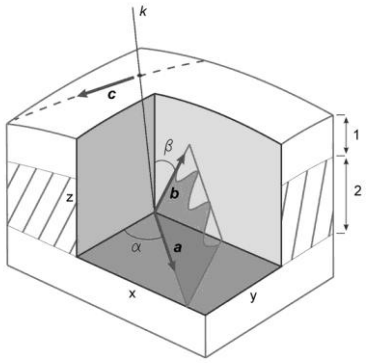

Figure 1. Definitions of angles of the dolphin skin structures, used for the calculation of the angle ϕ.

The angle β formed by the dermal papillae with the Z-axis as well as the vector normal to the fin surface was used for the calculation of a 3D vector ***b*** of the dermal papillae. Vectors ***a*** and ***b*** were used for the calculation of the local spatial

orientation of the plane of the dermal ridges in the data points (figure 1). The velocity vector ***c*** at the same points on the fin surface was used for the calculation of the angle ϕ between the plane of the dermal ridges and a line corresponding to the local flow direction:

$$\sin\varphi = \frac{\left|(y_b \cdot z_a - z_b \cdot y_a)x_c + (x_b \cdot z_a - z_b \cdot x_a)y_c + (x_b \cdot y_a - y_b \cdot x_a)z_c\right|}{\sqrt{(y_b \cdot z_a - z_b \cdot y_a)^2 + (x_b \cdot z_a - z_b \cdot x_a)^2 + (x_b \cdot y_a - y_b \cdot x_a)^2} \cdot \sqrt{(x_c^{\,2} + y_c^{\,2} + z_c^{\,2})}}$$

where ***a*** – ridges vector, ***b*** – papillae vector, and ***c*** – velocity vector.

Results

Hydrodynamics

The streamlined body of the common dolphin has a complex shape that resembles a body of revolution in the region from blowhole to the leading edge of the dorsal fin only. The head of the dolphin, especially the external morphology of the melon and the beak affects the flow and forms specific gradients of the velocity and pressure in that region. This part of the dolphin's body looks important in sense of flow control and formation of specific flow patterns around the dolphin body. The rear part of the dolphin's body, approximately 1/3 of the body length is flattened starting from the genital area to the tail flukes. To avoid the influence of natural turbulators like eye or blowhole, the position of the sampling line was defined to lie on the plane oriented at 45 degrees to the plane of symmetry of the dolphin body. This part of the body was found to show more homogeneous (i.e. less gradients in circumference direction), representative flow on the main body compared to other areas in the CFD simulation thus verifying the approach. For the dorsal fin the shape of the sampling line is close to a conventional airfoil shape. The cross-section of the dorsal fin made at the mid of the wing span is close to the NACA 63-015A and GOE 459 symmetrical airfoils. The main difference occurs at the thickened trailing edge of the fin.

The similarity in shape between fin and body section leads to a resemblance of gradients of the flow parameters in both regions (figure 2). The obvious difference in pressure gradient on the last third of the dolphin's body that associated with the strokes of the tail fin.

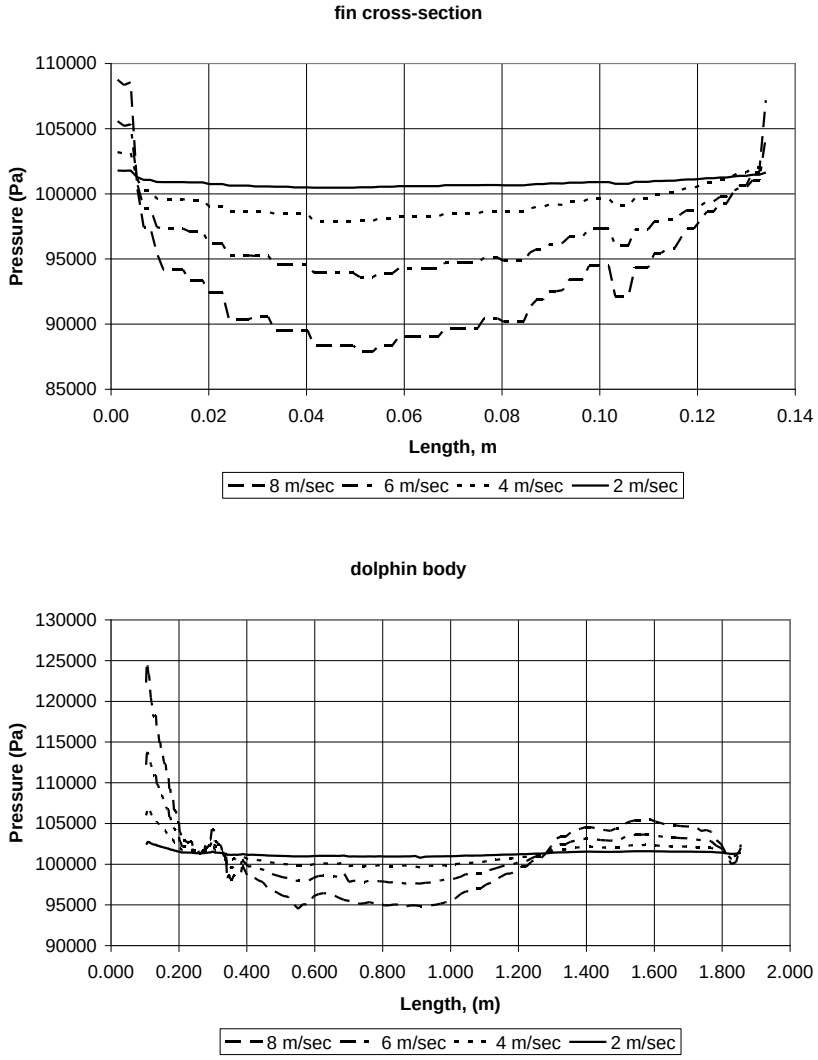

Figure 2. Pressure distribution along the cross-section of the dorsal fin (upper graphics) and body of the common dolphin (lower graphics) calculated for the range of dolphin swimming velocities.

The results of the flow simulations obtained with Floworks show a shift of the transition zone in frontward direction as well as a reduction of the laminar regions with increasing speed of swimming from 2 to 8 m/sec. For the minimal speed of swimming the laminar region on the upper part of the body reaches the dorsal fin position that corresponds approximately to the half of the body length. For the

maximal speed of 8 m/sec this region is reduced to the position of the pectoral fins that is less than one third of the body length.

While preliminary simulations in STAR-CCM+ with a low turbulence environment verified the above results, detailed study of the transition on the common dolphin model carried out by Riedeberger has shown that for the cruising speed of swimming around 3 m/sec in a moderate 1% turbulence-intensity environment the flow around the dolphin is mainly turbulent with limited laminar regions at the front of the head (figures 3, 4). The influence from the fin appendices on the main body pressure distribution was found to be of negligible impact. Estimations of possible surface drag reduction due to a downstream shift of transition were as high as 25 %.

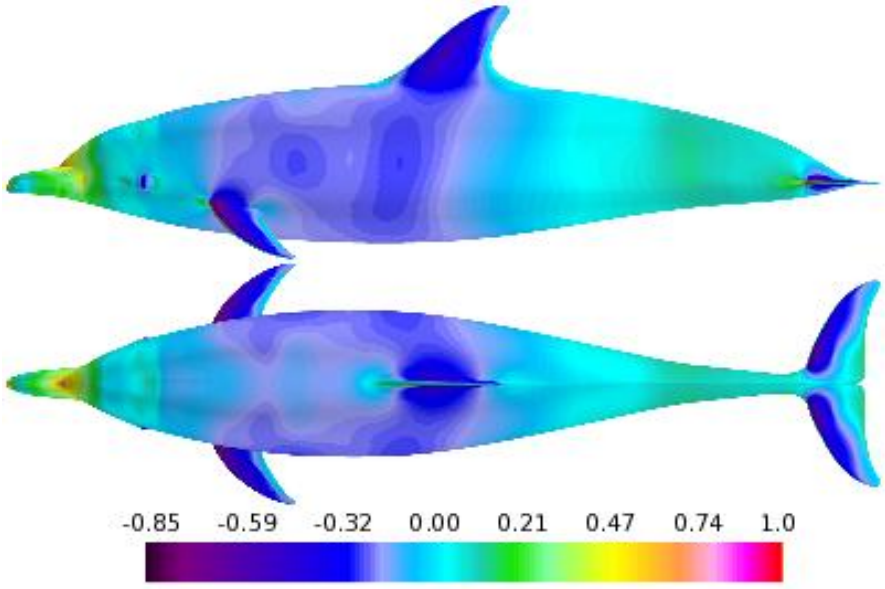

Figure 3. Distribution of pressure coefficient Cp for free-stream velocities of u_∞ = 1.0 m/s, side (upper) and top (lower) projection, turbulence intensity Tu = 1%

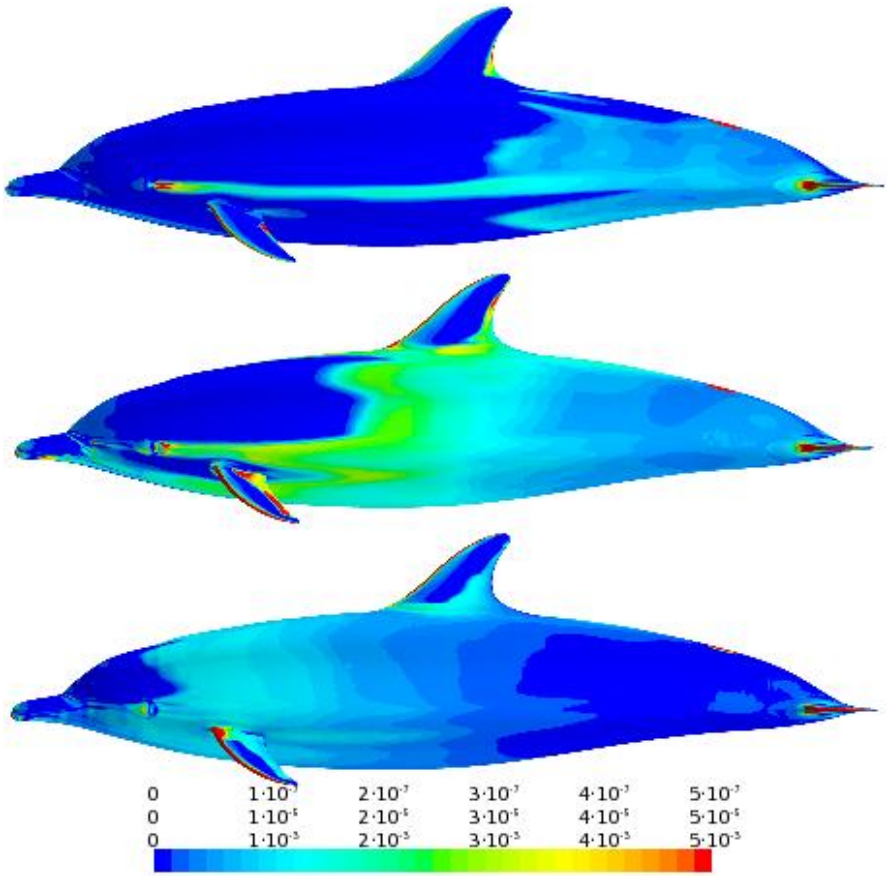

Figure 4. Turbulent kinetic energy k for free-stream velocities of u_∞ = 0.25 (upper), 1.0 (mid) and 2.5 m/s (lower), turbulence intensity Tu = 1%.

Skin morphology

Skin parameters of the common dolphin were compared in two locations, on the dorsal fin and on the body of the animal. Difference in mean values of thickness of dermis and epidermis ridges, height of the subpapillary layer, as well as angle ϕ was found significant at $p<0.05$. The significance of difference in mean values of the height of dermal papillary layer as well as total height of epidermis was found lower, at $p>0.05$.

A sketch of the different skin three-dimensional structures for both sampling lines is presented in Figure 5. The height of the composite upper layer of skin

which presents the biological analog on to an anisotropic compliant wall in engineering is similar at both locations. The difference in three-dimensional structure is related to the density and dimensions of the dermal ridges as well as their orientation with respect to the flow direction.

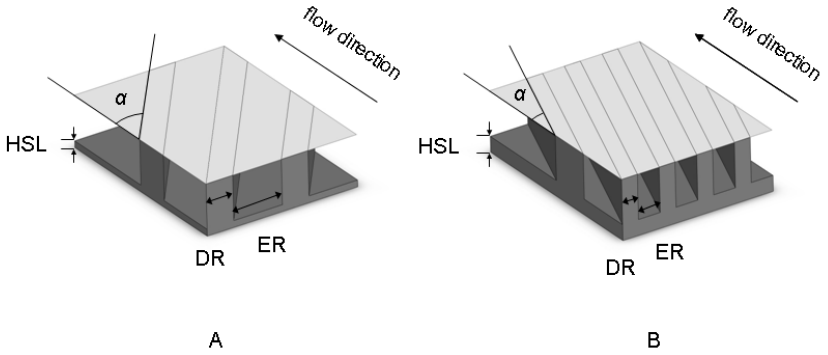

Figure 5. Sketch of three-dimensional structure of dolphin skin. A – on dorsal fin. B – along body.

At similar velocity gradient the distribution of the skin parameters is not uniform along the fin and the body of the dolphin. The skin parameters HEP, HDP, and HSL which make up the "compliant wall of the dolphin" correlate with the velocity gradient and smoothly decrease in caudal direction in both regions (figure 6). This relation stands out stronger for HEP and HDP and is weaker for the HSL parameter. Apart of that, the thickness both of dermal and epidermal ridges is negatively correlated with the chord-wise velocity distribution. This correlation is stronger on the dorsal fin compared with the body region.

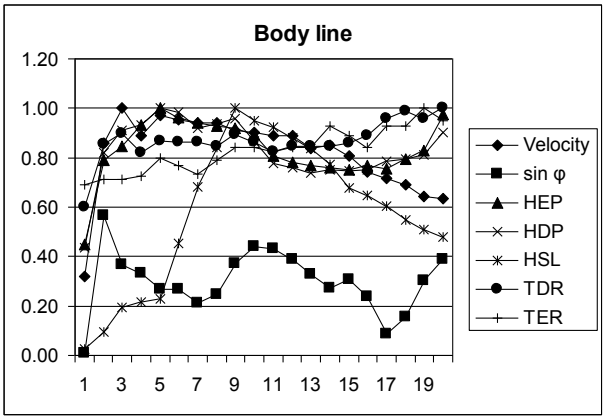

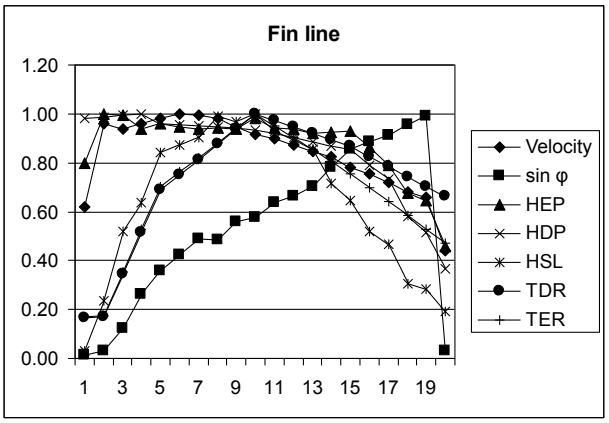

Figure 6. Variability of the flow and the skin structure parameters along two sampling lines. Data are normalized from 0 to 1.

Data obtained for the dorsal fin of the common dolphin can be compared with the previous results of the study for the dorsal fin of a harbor porpoise *Phocaena Phocaena*. As the cross-sections of the fins are close to conventional airfoils, the hypothesis of a possible relation between skin morphology parameters and derivatives of the functions of cross-sectional geometry was examined. For that purpose a curve fits of cross-sections of the dorsal fins were done with CurveExpert 1.4 by Daniel Hyams. The chord-wise thickness distribution Z(X) was interpolated by a 4th degree polynomial fit with the following coefficients for the common dolphin: a= -1.20E-03, b= 3.49E-03, c= -3.23E-04, d=1.12E-05, and e= -1.77E-07. For the cross-section of the harbor porpoise the appropriate coefficients were: a= -9.50E-01, b= 3.21E+00, c= -4.37E-01, d= 2.36E-02, and e= -4.79E-04.

For the common dolphin it was found that sin ϕ has *a* negative correlation with the 1st derivative of Z(X) function significant at $p<0.05$. This correlation revealed to be lower for the harbor porpoise. The difference in this correlation between two species is related with a less ordered arrangement of the dermal ridges on the dorsal fin of the harbor porpoise. The first two parameters of skin layer composition, HEP and HDP, have positive correlation with the 1st derivative of Z(X) significant at $p<0.05$ in both species, while for the HSL this correlation was found to be low.

Table 1. Correlations between skin morphology parameters and derivatives of the functions of cross-sectional geometry of the dorsal fin of common dolphin. Marked correlations are significant at $p < .05000$, N=20 (Casewise deletion of missing data).

	1st drv	2nd drv	Pressure	sin ϕ	HEP	HDP	HSL
1st drv	1.00	**-0.97**	-0.03	**-0.77**	**0.50**	**0.72**	-0.12
2nd drv	**-0.97**	1.00	-0.14	**0.82**	-0.30	**-0.54**	0.31
Pressure	-0.03	-0.14	1.00	-0.19	**-0.75**	**-0.56**	**-0.87**
sin ϕ	**-0.77**	**0.82**	-0.19	1.00	-0.09	-0.31	0.24
HEP	**0.50**	-0.30	**-0.75**	-0.09	1.00	**0.94**	**0.64**
HDP	**0.72**	**-0.54**	**-0.56**	-0.31	**0.94**	1.00	**0.50**
SPL	-0.12	0.31	**-0.87**	0.24	**0.64**	**0.50**	1.00

Table 2. Correlations between skin morphology parameters and derivatives of the functions of cross-sectional geometry of the dorsal fin of harbor porpoise. Marked correlations are significant at $p < .05000$, N=20 (Casewise deletion of missing data).

	1st drv	2nd drv	Pressure	sin ϕ	HEP	HDP	HSL
1st drv	1.00	**0.56**	**0.55**	-0.21	**0.67**	**0.80**	-0.08
2nd drv	**0.56**	1.00	-0.29	-0.44	**0.92**	**0.78**	**0.71**
Pressure	**0.55**	-0.29	1.00	0.08	-0.19	0.09	**-0.85**
sin ϕ	-0.21	-0.44	0.08	1.00	-0.25	-0.11	-0.19
HEP	**0.67**	**0.92**	-0.19	-0.25	1.00	**0.94**	**0.64**
HDP	**0.80**	**0.78**	0.09	-0.11	**0.94**	1.00	0.38
SPL	-0.08	**0.71**	**-0.85**	-0.19	**0.64**	0.38	1.00

Discussion

The challenge in biomimetics studies of natural phenomena is the complexity of the biological objects. As a rule, any biological structure is multifunctional by its nature and serves different functions. The main task in modeling of useful effects of a biological system is to reveal the variables that define the most part of the system behavior. In highly specialized systems showing an extremity in adaptation to (a) specific function(s), the number of significant variables can be limited, that helps in modeling the biological phenomenon. The dolphin skin differs from the skin of terrestrial mammals by an unusually ordered inner structure and a considerably simplified composition with reduced glands, hairs, and layers of the epidermis. These peculiarities of the dolphin skin were considered as adaptation to the life in the water which are potentially able to decrease the friction drag.

The choice of parameters relevant for the flow/skin interface is facilitated if one considers the dolphin skin as natural analogue of anisotropic compliant walls.

The latter have ordered inner structure and have a good potential in decreasing friction drag. In the general case, the wall matrix is reinforced by the aligned elements (fibers or voids) making the inner structure of the wall ordered [28]. The structure of the anisotropic wall is arranged so that rather than being displaced up and down by the fluctuating pressure it is displaced sideways as well making a substantial angle to the vertical, thereby generating a negative Reynolds shear stress on the compliant surface [30].

The first group of selected morphological parameters includes parameters of skin composition, i.e. the total height of the skin, as well as the height of two basic layers of skin. This corresponds to the basic design of a two-layer anisotropic compliant wall by Carpenter. The angle ϕ presents the angle between flow direction and dermal ridges as an analogue to the ordered elements in the compliant wall matrix. The second group of parameters consists of the thickness of the ordered elements and distance between them. The parameters of this group can be considered as the next step from the two-dimensional case of an anisotropic compliant wall to the more complex three-dimensional one.

For a better understanding the correlations between local flow parameters and skin structure at two different locations having similar shape but different Reynolds numbers, i.e., the body and dorsal fin of the dolphin, were compared. Additionally, the results for the dorsal fin were compared with the previously obtained data for the harbor porpoise. The last comparison aimed to reveal possible differences in the flow/skin interface in fast-swimming (common dolphin) and low-swimming (harbor porpoise) species.

The data obtained show obvious correlations between parameters of the two-dimensional skin composition and relative gradients of the velocity and pressure. This correlation was found similar for the dolphin body and the fin, having different ranges of Re number. A similar relationship was also observed for the parameters of the three-dimensional structure of the skin. Apart from that, the relation between the angle ϕ and pressure and velocity gradients was found to be non-linear.

The results of this study allow to conclude that the stream-wise variability of the dolphin skin structure appears to be associated with the streamlined body geometry and corresponding gradients of the velocity and pressure rather than with specific local Re numbers. The difference in results for the dolphin's body and cross-section of the dorsal fin can be related to the degree of specialization of these two regions. The dorsal fin having a wing-like shape presents an extremum in hydrodynamic function while the fin cross-sections are close to conventional symmetrical airfoils. Apart from the body region, the relation between airfoil geometry and surface structure is presented clearer there. All morphological pa-

rameters including the angle ϕ correlate with the 1st derivative of the interpolated cross-sectional geometry.

Comparison of this correlation between common dolphin and harbor porpoise has shown that it is stronger for the first species. This distinction could reflect the difference in hydrodynamic performance, as the common dolphin is recognized to be a fast swimmer, while the harbor porpoise has an approximately half as large average-speed of swimming. To check if the difference in the flow/skin interface refers to the potential drag reduction rather than the taxonomic features, an additional study of species with different swimming performance is needed.

Theoretical and experimental studies of compliant walls have shown that drag can be minimized by delaying the transition from laminar to the turbulent flow and by stabilization of the turbulent flow in the boundary layer. Potentially, a dolphin skin close to the anisotropic compliant wall design could reduce the friction drag in both ways. Meanwhile, the potential drag-reducing effect depends considerably on the external flow conditions, such as initial flow velocity and turbulence level.

A general question of possible friction-drag reduction by the skin of a swimming dolphin can be posed as follows: Which flow conditions is it optimized for? Dolphins use a variety of swimming speeds and modes, the cruising speed is normally within the range of 1-4 m/sec, while the top speed of the burst can reach up to 8-10 m/sec. During swimming the active phase can be interspersed with gliding phases which anticipate different flow regimes and mechanisms of boundary-layer stabilization.

From the point of view of optimization of energy expenditures, two hypotheses on potential drag-reducing properties of dolphin skin can be proposed. The first assumes that the skin is optimized for the cruising motion with moderate speed of swimming 1-4 m/sec in low depth with relatively high initial turbulence. The fact, that dolphins spend most of their time moving with moderate speed speaks in favor of this supposition. An alternative hypothesis, based on the “cheetah hunting strategy” [33], anticipates extreme energy expenditure for a short-time period with a chance to catch a prey and compensate energy losses. Following this idea, the dolphin skin could be optimized for the reduction of friction drag during fast swimming at moderate or high depth with relatively low initial turbulence.

Outlook

The next step in the study of the flow/skin interface in dolphins is getting the complete distribution of skin morphology and flow parameters all over the body of the dolphin. The complex geometry of dolphins presents a variety of specific local flow conditions that gives an opportunity to verify the relation between skin struc-

ture and local flow parameters obtained in the ongoing study. An important prerequisite for a future study is the variability of the swimming performance and Re numbers of different species that allows carrying out comparative studies of the potential drag-reducing properties of dolphin skin.

From the point of numerical simulation the next steps would include a more detailed understanding of the marine turbulent environment to more accurately account for the reality in simulation boundary conditions. Furthermore unsteady effects on transition location due to swimming body motion would enable more insight to the phenomena whereas a comparative study of the possibilities of available turbulence modeling approaches can shed more insight in the limitations of simulation and in the end enable more precise answers to drag-reduction capabilities of modeled compliant walls.

Acknowledgements

Our thanks go to Dr. Vincent, Dr. Dabin, Dr. Doremus, and Dr. Jensen for their help with dolphin morphology, and to the staff of the Labor für Orthopädie und Biomechanik for their help with laser scanning the dolphin model. We also thank Dr. Benke for the opportunity to work on a dolphin model in the German Oceanographic Museum in Stralsund.

Literature

[1] Gray J. 1936. “Studies in Animal Locomotion VI. The Propulsive Powers of the Dolphin” J. Exp. Biol. 13: 192-199.

[2] Kramer M. O. 1960a. “Boundary Layer Stabilization by Distributed Damping,” J. Amer. Soc. Nav. Eng. 72: 25–33.

[3] Kramer M. O. 1960b. “The Dolphins' Secret,” New Sci., 7: 1118–1120.

[4] Sokolov V.E. 1973. Integument of mammals. Moscow: Nauka (in Russian).

[5] Sokolov V.E. 1960. “Some Similarities and Dissimilarities in the Structure of the Skin Among the Members of the Suborders Odontoceti and Mystacoceti (Cetacea),” Nature 185: 745–747.

[6] Parry D. A. 1949a. “The Swimming of Whales and a Discussion of Gray's Paradox,” J. Exp. Biol. 26: 24–34.

[7] Aleyev Y. G. 1977. Nekton. Junk, The Hague, Netherlands.

[8] Haun J. E., E. W. Hendricks F. R. Borkat R. W. Kataoka D. A. Carder and N. K. Chun. 1983. “Dolphin Hydrodynamics: Annual Report FY 82.” NOSC* TR935. SSC San Diego, CA.

[9] Pershin S.V. 1988. Fundamentals of hydrobionics. Leningrad: Sudostroyeniye (in Russian).

[10] Toedt M.E., Reuss L.E., Dillaman R.M., Pabst D.A. 1997. “Collagen and elastin arrangement in the blubber of common dolphin (Delphinus delphis)”. Am Zool 37: 56A.

[11] Hamilton J. L., W. A. McLellan and D. A. Pabst. 1998. “Functional Morphology of Harbor Porpoise (Phocoena phocoena) Tailstock Blubber,” Amer. Zool. 38: 203A.

[12] Palmer E., Weddell G. 1964. “The relation between structure, innervation and function of the skin of the bottlenose dolphin (Tursiops truncatus)”. Proc Zool Soc Lond 143: 553–568.

[13] Purves P. E. 1969. “The Structure of the Flukes in Relation to Laminar Flow in Cetaceans” Z. Sдugertierkd. 34: 1-8

[14] Surkina R.M. 1971. “Structure and function of the skin muscles of dolphins”. Bionika 5: 81–87 (in Russian).

[15] Babenko V.V., Koslov L.F., Pershin S.V., Sokolov V.Ye., and Tomilin A.G. 1982. “Self-adjustment of Skin Dampening in Cetaceans in Active Swimming,” Bionika 16: 3–10 (in Russian).

[16] Babenko V.V. 1979. “Investigating the Skin Elasticity of Live Dolphins,” Bionika 13: 43–52 (in Russian).

[17] Pabst D.A., McLellan W.A., Gosline J.G., and Piermarini P.M. 1995. “Morphology and Mechanics of Dolphin Blubber,” Amer. Zool. 35: 44A.

[18] Romanenko E.V. 2002. Fish and Dolphin Swimming (Sofia: Pensoft)

[19] Rohr, J., Latz M. I., Fallon S., Nauen J.C, and Hendricks E.W. 1998. “Experimental Approaches Towards Interpreting Dolphin-stimulated Bioluminescence” J. Exp. Biol. 201: 1447–1460.

[20] Haider M. and Lindsley D. B. 1964. “Microvibrations in Man and Dolphin” Science 146: 1181–1183.

[21] Ridgway S. H. and Carder D. A. 1993. “Features of Dolphin Skin with Potential Hydrodynamic Importance,” IEEE Eng. Med. Biol. 12: 83–88.

[22] Babenko V.V., and Carpenter P.W. 2003. “Dolphin hydrodynamics Flow Past Highly Compliant Boundaries and in Collapsible Tubes” ed P.W. Carpenter and T. J. Pedley (Dordrecht: Kluwer) pp 293–323, chapter 13.

[23] Nagamine H., Yamahata K., Hagiwara Y. and Matsubara R. 2004. ”Turbulence modification by compliant skin and strata-corneas desquamation of a swimming dolphin” J. Turb. 18: 1–25.

[24] Gad-el-Hak M. 1996. “Compliant coatings: a decade of progress” Appl. Mech. Rev. 49: 147–57.

[25] Choi K.S., Yang X., Clayton B.R., Glover E.J., Atlar M., Semenov B.N., and Kulik V. M. 1997. “Turbulent drag reduction using compliant surfaces” Proc. R. Soc. A 453: 2229–40.

[26] Sokolov V.E. 1955. “Structure of the integument of some cetaceans” Byulleten’ Moskovskogo obshestva Ispitatelej prirodi Otdel biologii 60: 45–60 (in Russian).

[27] Carpenter P.W., Davies C. and Lucey A.D. 2000. “Hydrodynamics and compliant walls: does the dolphin have a secret?” Curr. Sci. 79: 758–65.

[28] Grosskreutz R. 1971. „Wechselwirkungen zwischen turbulenten Grenzschichten und weichen Wanden“, MPI fьr Strцmungsforschung und der AVA Göttingen Mitt. 53.

[29] Stromberg M.W. 1989. “Dermal–epidermal relations in the skin of bottlenose dolphin (Tursiops truncatus)” Anat. Histol. Embryol. 18: 1–13.

[30] Carpenter P.W. and Morris P.J. 1990. “The effect of anisotropic wall compliance on boundary-layer stability and transition” J. Fluid Mech. 288: 171–223.

[31] Yeo K.S. 1990. “The hydrodynamic stability of boundary-layer flow over a class of anisotropic compliant walls” J. Fluid Mech. 220: 125–60.

[32] Riedeberger D., U. Rist. 2011. Numerical simulation of laminar-turbulent transition on a dolphin using the γ-Re_θ model. In High performance computing in science and engineering ’11 : transactions of the High Performance Computing Center, Stuttgart (HLRS), Nagel, Wolfgang E.; Kröner, Dietmar B.; Resch, Michael M. (Eds.) (Berlin,London: Springer, 2011).

[33] Aguilar Soto, N., M. P. Johnson, P. T. Madsen, F. Diaz, I. Dominguez, A. Brito and P. Tyack. 2008. Cheetahs of the deep sea: Deep foraging sprints in short-finned pilot whales off Tenerife (Canary Islands). Journal of Animal Ecology 77:936–947.